# An Examination of ATO J031.2309+52.9923, a δ Scuti Variable from the ATLAS Survey

**Eric G. Hintz**
**Jarrod L. Hansen**
**Denise C. Stephens**
**Benjamin J. Derieg**
*Department of Physics and Astronomy, Brigham Young University, N283 ESC, Provo, UT 84602; hintz@byu.edu*

*Received June 1, 2022; revised July 29, 2022; accepted July 29, 2022*

**Abstract** As part of our variable star follow-up program we have examined a number of stars from the ATLAS (Asteroid Terrestrial-impact Last Alert System) survey. The first of these, ATO J031.2309+52.9923, was reported with a period of 0.069705 d. Our revised period is 0.06970555 d, but we find an additional period of 0.074 d. We also report a suspected period change of $(1/P)\,dP/dT = -340 \times 10^{-8}\,yr^{-1}$. In addition to the primary period, we find two additional closely spaced periods of 0.07380 d and 0.07338 d, with a period ratio of $P_1/P_2 = 0.945$. The period ratio and change would indicate that this object is a δ Scuti variable with non-radial pulsations. We find that this target fits into the medium amplitude group of δ Scuti variables such as AN Lyncis.

## 1. Introduction

There are a large number of surveys that generate light curves, such as ATLAS (Asteroid Terrestrial-impact Last Alert System), which is looking for asteroids which could potentially hit the Earth. There is also ASAS-SN, which is looking for supernova events. Then there are systems like TESS that are looking for transiting planets. Finally, we are near the advent of LSST. In all these cases light curves of short period pulsating stars are generated. However, in many cases the cadence is not ideal for objects such as δ Scuti variables, with the TESS 2-minute cadence observations being an obvious exception.

As part of our campus observing program we selected a number of potential δ Scuti stars to examine at a higher cadence. We started with the ATLAS database of potential variables (Heinze *et al.* 2018). We selected objects from their lists of PULSE and MPUL objects for more detailed follow-up studies. One of the first targets selected was one we label as ATLAS 30 from our own internal numbering system. This target is designated ATO J031.2309+52.9923 in the ATLAS survey and had an estimated period of 0.069705 d. It is located at R.A. (2000) $02^h\ 04^m\ 55.4^s$, Dec. (2000) +52° 59' 32.6". This object is also found in the ASAS-SN (Shappee *et al.* 2014; Kochanek *et al.* 2017) archive (ASASSN-V J020455.45+525932.6), where it is listed as a High Amplitude δ Scuti (HADS) with a period of 0.0697056 d. In the TESS archives the target is TIC 250510098. From the 2MASS (02045542+5259325) and AllWISE (J020455.43+525932.5) surveys we find (Cutri *et al.* 2003, 2014):

J = 11.409 ± 0.025,
H = 11.273 ± 0.023,
K = 11.221 ± 0.022,
W1 = 11.186 ± 0.023,
W2 = 11.204 ± 0.021,
W3 = 11.193 ± 0.165,
W4 = 9.1.

From the Gaia EDR3 release (Bailer-Jones *et al.* 2021) we have a distance of 1,004 pc. Given galactic coordinates of l = 133.9849° and b = –8.2951°, this puts ATLAS 30 within the disk. From a Gaia DR2 reduction of surface temperatures Bai *et al.* (2019) we deduce a temperature for ATLAS 30 of 7430 ± 214 K. In the *TESS Input Catalogue* 34 (Stassun *et al.* 2019) they report a number of values: a temperature of 7728 ± 08 K, log g = 4.01 ± 0.10, [M/H] = –0.34 ± 0.02, and $M = 1.82\,M_\odot$. All these values point to ATLAS 30 being a late A dwarf, which is in line with a δ Scuti designation. The metal content is a bit surprising given the star's location in the disk.

Since ATLAS 30 is potentially a new δ Scuti variable we examined some basic information on the varieties of δ Scuti that exist. In Breger and Pamyatnykh (1998) they discuss the period changes seen in three groups of δ Scuti variables, Pop. I radial pulsators, Pop. I non-radial pulsators, and Pop. II radial pulsators. For all the radial pulsators they find changes in $(1/P)\,dP/dt$ to be in about the $\pm 10 \times 10^{-8}\,yr^{-1}$ range. For the non-radial pulsators they list changes 10x greater. For example, XX Pyx has a period change value for the primary period of $340 \times 10^{-8}\,yr^{-1}$ 41 (Handler *et al.* 1998) and $-110 \times 10^{-8}\,yr^{-1}$ for 4 CVn (Breger 1990). In addition, Breger and Pamyatnykh (1998) provide the first and second period for a number of radial and non-radial pulsators. For two radial pulsators they found $P_1/P_2 = 1.302$ for AI Vel and $P_1/P_2 = 1.279$ for SX Phe. From Handler *et al.* (1998) we find $P_1/P_2 = 0.929$ for XX Pyx.

In this paper we will present an O–C period determination for this potential new δ Scuti, along with a potential period change. A Fourier decomposition of the light curve will also be reported, and examined in each of the various seasons to provide all significant frequencies in the data.

## 2. Photometric data

### 2.1. Robotic observations

Beginning in 2019 we secured data on ATLAS 30 using a group of robotic telescopes mounted on the observation deck of the Eyring Science Center at Brigham Young University.

Table 1. Telescope and CCD specifications.

| *Telescope* | *CCD* | *Pixel Size (μm)* | *Plate Scale ("/pixel)* | *Nights* | *Years* |
|---|---|---|---|---|---|
| TPO 12" | FLI ML8300 | 5.4 | 0.46 | 5 | 2021–2022 |
| Vixen VMC200L | FLI ML3200 | 6.8 | 0.72 | 59 | 2019–2021 |
| Vixen VMC200L | FLI ML8300 | 5.4 | 0.57 | 9 | 2022 |
| Takahashi Mewlon-250 | FLI ML8300 | 5.4 | 0.37 | 21 | 2019 |

Table 2. Comparison star values.

| *Star No.* | *Name* | *R.A. (2000) h m s* | *Dec. (2000) ° ′ ″* | *B* | *V* |
|---|---|---|---|---|---|
| 1 | TYC 3685-1001-2 | 02 05 01.1 | +53 00 05.6 | 12.06 | 11.47 |
| 2 | TYC 3685-489-1 | 02 05 07.6 | +52 59 43.0 | 11.90 | 11.53 |
| 3 | TYC 3685-2151-1 | 02 05 32.8 | +53 06 12.8 | 13.72 | 12.05 |
| 4 | TYC 3685-2252-1 | 02 05 48.2 | +53 06 27.2 | 12.79 | 12.01 |
| 5 | TYC 3685-2211-1 | 02 04 57.0 | +53 06 02.4 | 12.86 | 12.18 |
| 6 | TYC 3685-225-1 | 02 05 08.0 | +52 54 52.1 | 12.52 | 12.12 |

The overall facility is known as the Orson Pratt Observatory. This facility is located at an elevation of 1,430.4 m with moderately dark skies. We used three telescopes to secure data on 94 nights. The telescope configurations are given in Table 1, along with the number of nights for each configuration. For all but three nights of observing, the data were obtained through a Johnson V filter. The remaining three nights were taken with a Johnson B filter. All observations were reduced using standard IRAF procedures.

Each night's data were then processed through AstroImageJ (Collins *et al.* 2017) to generate light curves, using comparison stars to provide calibrated magnitudes. The area around our target star is shown in Figure 1 with the comparison stars marked. Information on the comparison stars is gathered in Table 2. None of the comparison stars are flagged as potentially variable in any survey and after a careful check we find no significant variations. We do note that there is a faint star to the East of ATLAS 30, however given our aperture choice we do not feel this star ever contributed light to our measurements. A sample of one of the longer nights of data is shown in Figure 2.

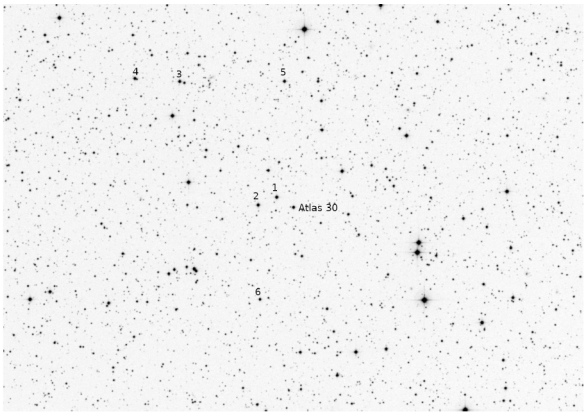


Figure 1. Field of ATO J031.2309+52.9923 (labeled ATLAS 30) with comparison stars labeled.

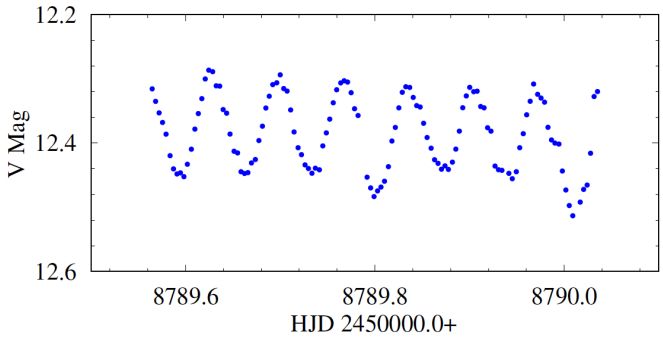


Figure 2. A long night of data from JD 2458789.

## 2.2. Archival photometry

In addition to our own data we gathered observations from three main archives. First we downloaded all the data from the ATLAS program (Heinze *et al.* 2018) using the NASA MAST archive. These observations are in two filters, c (140 observations) and o (154 observations). Those are effectively cyan and orange filters that cannot be directly matched to our data sets. We then did a search for the last 3,000 days within the ASAS-SN archive (Shappee *et al.* 2014; Kochanek *et al.* 2017). Data from AS-SN can be either in V (571 observations) or g (1315 observations). In this case we can add the V observations directly to our data set. Finally we downloaded the data from the TESS archive. These data come from a fairly wide filter centered roughly in the I band. From here we gathered 993 observations.

Table 4. Frequency content of ATO J031.2309+52.9923 from TESS data.

| | *Frequency c d$^{-1}$* | *Amplitude mag.* | *Phase* | *S/N* |
|---|---|---|---|---|
| $f_1$ | 14.34546(7) | 0.0452(1) | 0.4869(5) | 253 |
| $f_2$ | 13.5498(7) | 0.0048(1) | 0.886(4) | 27 |
| $2f_1$ | 28.693(1) | 0.0022(1) | 0.925(9) | 16 |
| $f_3$ | 13.629(1) | 0.0021(1) | 0.72(1) | 12 |

Table 3. Times of maximum light for ATO J031.2309+52.9923.

| *Cycle* | *HJD 2450000.0+* | *O–C* | *Filter* |
|---|---|---|---|
| 0 | 8522.65095 | –0.00232 | V |
| 1 | 8522.71969 | –0.00328 | V |
| 57 | 8526.62671 | 0.00023 | B |
| 57 | 8526.62481 | –0.00167 | V |
| 58 | 8526.69606 | –0.00013 | B |
| 229 | 8538.61579 | –0.00005 | V |
| 230 | 8538.68528 | –0.00026 | V |
| 272 | 8541.61370 | 0.00052 | V |
| 273 | 8541.68287 | –0.00001 | V |
| 273 | 8541.68231 | –0.00057 | B |
| 459 | 8554.65007 | 0.00195 | V |
| 2873 | 8722.91750 | 0.00018 | V |
| 2888 | 8723.96282 | –0.00008 | V |

*Note: Table 3 is published in its entirety in the machine-readable format. A portion is shown here for guidance regarding its form and content. Full table available at: ftp://ftp.aavso.org/public/datasets/3838-Hintz-atoj031.txt.*

## 3. Analysis

### 3.1. Times of maximum light

The first stage of the analysis was to obtain times of maximum light from all light curves with sufficient coverage. This was done using using Peranso (Paunzen and Vanmunster 2016). We used a third order fit to each maximum and then obtained the time of maximum from the fit. We determined 176 times of maximum light, 173 in the V filter and 3 in the B filter. All these times are gathered in Table 3. Using only the times for the V filter we determined an ephemeris of:

$$HJD_{max} = 2458522.65327(23) + 0.069705552(28)E \quad (1)$$

The errors included are for the last two digits of both the period and starting epoch. Using this equation we determined calculated times of maximum light and O–C values for each maximum. These are also gathered into Table 3. In Figure 3 we show the O–C diagram for ATLAS 30. Since there appeared to be a slight bowing to the curve we determined a second order fit as given in:

$$HJD_{max} = 2458522.65217(41) + 0.06970593(12)E - 2.24(70) \times 10^{-11}E^2 \quad (2)$$

This is right at the edge of a 3σ detection for a period change. Continued coverage of this object would be needed to determine if the period change is real. Using the standard method of reporting period change we found $(1/P)(dP/dt) = -340 \times 10^{-8}\,yr^{-1}$. This is similar to the value found for XX Pyx by Handler *et al.* (1998), although it is negative. As mentioned earlier, a detailed discussion of period changes in δ Scuti variables can be found in Breger and Pamyatnykh (1998). If the detected period change is real it would indicate that ATLAS 30 is likely a non-radial pulsator.

Another interesting result from the O–C analysis has to do with patterns in the residuals. On a number of nights in November 2019 we found 5 to 7 maxima per night. This allowed us to examine cycle-to-cycle changes in the O–C values and the shapes of the light curves. As seen in Figure 4, there appears to be a potential periodic change in the O–C values. Using O–C data over 25 days from this time period, we used Peranso and found a frequency at $f_b = 0.794\,c\,d^{-1}$ that phased these O–C values. There was also a nearby peak at $f_a = 0.719\,c\,d^{-1}$, as shown in Figure 5. The lower panel in Figure 5 shows the phased O–C values using the $f_b$ value. These values will be discussed further in the next section.

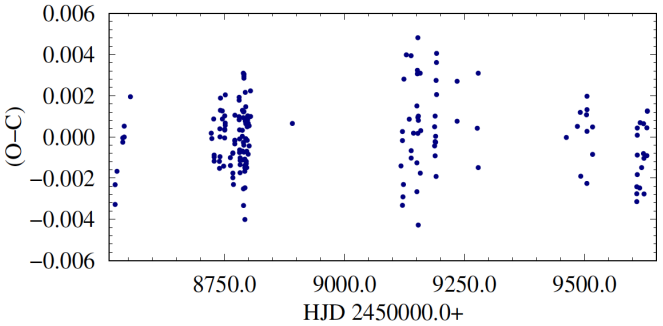


Figure 3. O–C Diagram from 174 times of maximum light from 2019 to 2022.

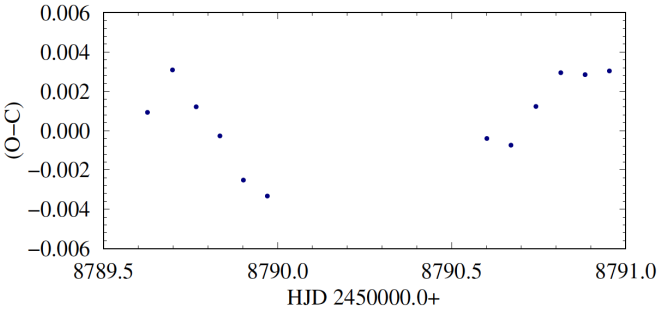


Figure 4. O–C Diagram for two consecutive nights in November 2019.

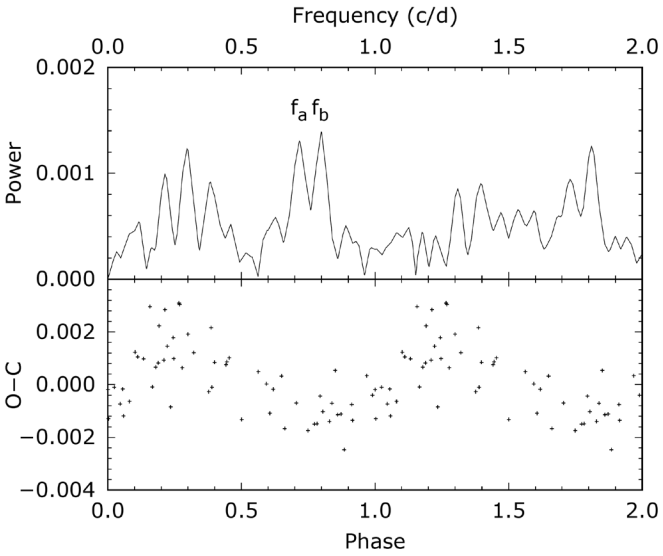


Figure 5. The upper panel is the power spectrum of the O–C values from November of 2019. The lower panel shows the phased O–C values for a frequency of 0.794 c $d^{-1}$.

3.2. Fourier decomposition

To begin our Fourier analysis we sorted long runs of data into sets based on gaps in the data. This allows for an examination of period and amplitude changes over time and reduces some aliasing. To perform our initial decomposition we used Period04 (Lenz and Breger 2005). From the TESS data we found a solution with frequencies as reported in Table 4. The S/N for the four reported frequencies are well above the cut-off suggested by Lenz and Breger (2005), but no other frequencies reach this level. We note that the filter system for TESS is a fairly wide filter centered near the traditional I filter. The one concern with the TESS data is the low Nyquist frequency of 24.0028 c/d. In Figure 5 we show the power spectrum for the original data set and with the first frequency removed. In the top graph we can see the primary frequency at 14.345 c d$^{-1}$, but we see another at 33.661 c d$^{-1}$. That is mirrored around the Nyquist frequency.

The value for $2f_1$ is a little above the Nyquist frequency, so there is some concern. In the lower panel of Figure 6 we see $f_2$ and $2f_1$. We also see the mirrored frequencies. For typical HADS, which have a fast rise that needs to be fit with a number of harmonics of the primary frequency, we would have more issues with this mirroring effect. However, given that ATLAS 30 has a more symmetric curve, the low Nyquist frequency doesn't have as much of an impact.

To further examine the frequency content of ATLAS 30 we split our own data set into two groups, one before JD2459000 and one after. This provided a much higher Nyquist frequency of approximately 135 c d$^{-1}$. For the data set before JD2459000 we found the power spectrum shown in Figure 7. This shows the typical power spectrum from a single location, without the mirroring effect. To confirm our frequency content we used the CLEANest method (Foster 1995) found in Persano. The same four frequencies were recovered. Although we don't find significant frequencies at $f_1$–$f_2$ and $f_1$–$f_3$ in the Fourier analysis, we note that these values of 0.795 and 0.716 are the same as the values found for the changes in O–C values. Therefore any sinusoidal changes seen in the O–C values are related to the beating of two frequencies, not from an orbital motion. We also note a period ratio of $P_1/P_2 = 0.945$ from our frequency solution.

When running a Period04 solution on the various data sets we found a different number of the primary frequencies listed above. For both the cyan and orange data sets from ATLAS we only recovered the primary frequency. This is also true of an analysis of the ASAS-SN g filter data. For the ASAS-SN V filter data we found $f_1$ and $2f_1$, but not the additional frequencies. From our largest seasonal data sample from 2019 we recovered the first three frequencies.

Using the four frequencies from Table 4 we examined various subsets of data from all sources. A primary focus here was on the V$ filter data from ASAS-SN and our observations. We find that the amplitude of the primary frequency has slowly increased over time from about 0.145 to 0.155 (see Figure 8). Knowing this slight change allows us to compare the amplitude in different spectral ranges for the same epoch. The ATLAS c filter has broad coverage from 420 nm to 650 nm and has an amplitude similar to the V filter at a common time. The ATLAS o filter covers a range of the Sloan r and i together. At JD 2457600

Table 4. Frequency content of ATO J031.2309+52.9923 from TESS data.

| | *Frequency* c d$^{-1}$ | *Amplitude* mag. | *Phase* | *S/N* |
|---|---|---|---|---|
| $f_1$ | 14.34546(7) | 0.0452(1) | 0.4869(5) | 253 |
| $f_2$ | 13.5498(7) | 0.0048(1) | 0.886(4) | 27 |
| $2f_1$ | 28.693(1) | 0.0022(1) | 0.925(9) | 16 |
| $f_3$ | 13.629(1) | 0.0021(1) | 0.72(1) | 12 |

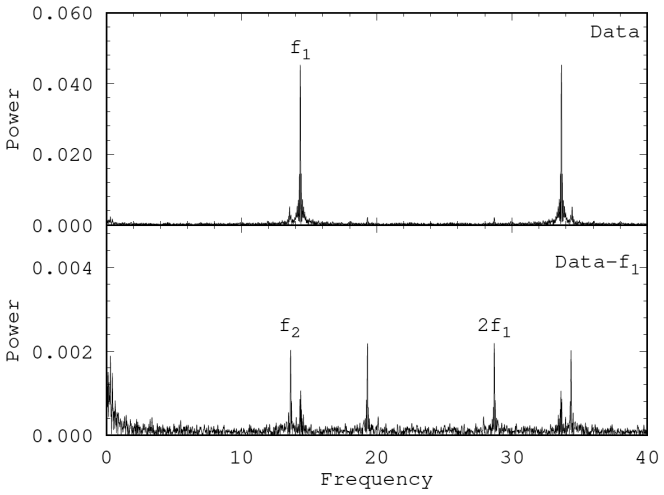


Figure 6. Fourier Spectrum from TESS data from Period04.

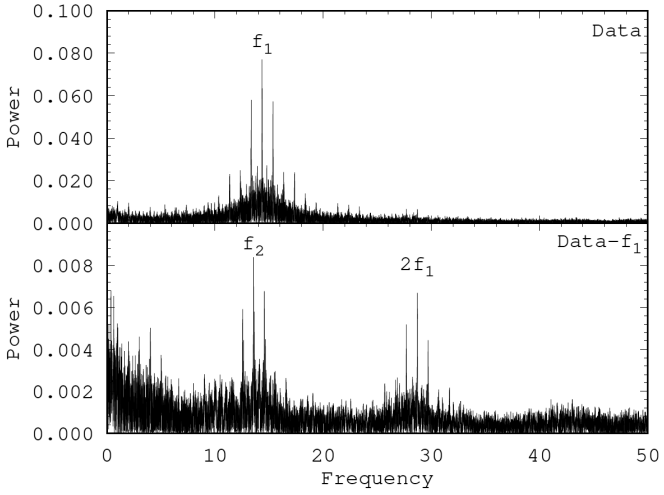


Figure 7. Fourier Spectrum from BYU data prior to JD2459000 from Period04.

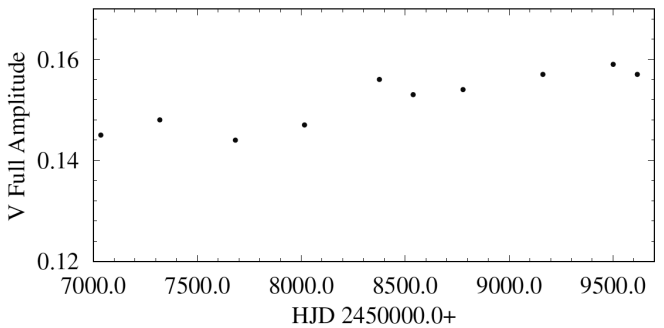


Figure 8. Full amplitude of the primary frequency as a function of time.

we find an amplitude of 0.144 in the V filter compared to 0.121 in the ATLAS o filter. At JD2458800 we have a V amplitude of 0.154 and a TESS amplitude of 0.091. Finally, we compare the ASAS-SN g observations with an amplitude of 0.173 to the V amplitude of 0.157. In all cases the bluer filter shows the higher amplitude that is normal for pulsating variable stars.

## 4. Conclusion

After an analysis of ATLAS 30 (ATO J031.2309+52.9923) we find that it is a non-radial δ Scuti variable with a fundamental frequency of f= 14.34546 c d$^{-1}$, or a period of 0.069705552 d. In addition, there is some evidence that this star is experiencing a period change of $(1/P)(dP/dt) = -340 \times 10^{-8}$ yr$^{-1}$. This is similar to values found for non-radial δ Scuti variables from previous publications. However, the detection of a period change is right at the 3σ level and will need to be confirmed by additional observations. A second period is also found at 0.073801 d. This gives a period ratio of $P_1/P_2 = 0.945$, which is similar to that found by Handler *et al.* (1998) for XX Pyx, which is a non-radial pulsator. Radial pulsators tend to have period ratios greater than 1.

An examination of all available data sets shows that the ATLAS data were able to accurately determine the primary frequency, but didn't recover the additional frequencies reported here. Therefore, those data alone could not fully characterize the object. The case was the same for g data from the ASAS-SN program. While the V data did recover the first harmonic ($2f_1$), they did not recover the two additional frequencies. Our high density data and the consistent data from TESS both recovered four clear frequencies.

We find that while the ASAS-SN program has labeled this star as a high amplitude δ Scuti, it really doesn't fit that characterization. The average amplitude in the V filter of 0.150 is below the general cut-off for HADS and the light curve shape isn't typical. The object also doesn't fall into the LADS category with amplitudes below 0.1. This object is typical of the in-between group of objects that have medium amplitudes such as AN Lyncis (Rodriguez *et al.* 1997; Zhou *et al.* 2017). Perhaps the best description is a medium amplitude δ Scuti, as it is called by Rodriguez *et al.* (1997).

## 5. Acknowledgements

We acknowledge the Brigham Young University, Department of Physics and Astronomy for their continued support of our research efforts. We wish to thank Maureen Hintz for her editorial help. We acknowledge a grant from the Theodore H. Dunham Fund for Astrophysical Research which has been used to help equip the BYU campus observatory. This research was also supported in part by NASA through the American Astronomical Society's Small Research Grant Program.

This publication makes use of data products from the Wide-field Infrared Survey Explorer, which is a joint project of the University of California, Los Angeles, and the Jet Propulsion Laboratory/California Institute of Technology, funded by the National Aeronautics and Space Administration. This publication makes use of data products from the Wide-field Infrared Survey Explorer, which is a joint project of the University of California, Los Angeles, and the Jet Propulsion Laboratory/California Institute of Technology, funded by the National Aeronautics and Space Administration. This publication makes use of data products from the Two Micron All Sky Survey, which is a joint project of the University of Massachusetts and the Infrared Processing and Analysis Center/California Institute of Technology, funded by the National Aeronautics and Space Administration and the National Science Foundation.

Facilities: TESS,MAST,BYU:0.2m,BYU:0.3m

## References

Bai, Y., Liu, J., Bai, Z., Wang, S., and Fan, D. 2019, *Astron. J.*, **158**, 93.

Bailer-Jones, C. A. L., Rybizki, J., Fouesneau, M., Demleitner, M., and Andrae, R. 2021, *Astron. J.*, **161**, 147.

Breger, M. 1990, *Astron. Astrophys.*, **240**, 308.

Breger, M. and Pamyatnykh, A. A. 1998, *Astron. Astrophys.*, **332**, 958.

Collins, K. A., Kielkopf, J. F., Stassun, K. G., and Hessman, F. V. 2017, *Astron. J.*, **153**, 77.

Cutri, R. M., *et al.* 2003, VizieR Online Data Catalog: 2MASS All-Sky Catalog of Point Sources (2003yCat.2246....0C).

Cutri, R. M., *et al.* 2014, VizieR Online Data Catalog: AllWISE Data Release (2014yCat.2328....0C).

Foster, G. 1995, *Astron. J.*, **109**, 1889.

Handler, G., Pamyatnykh, A. A., Zima, W., Sullivan, D. J., Audard, N., and Nitta, A. 1998, *Mon. Not. Roy. Astron. Soc.*, **295**, 377.

Heinze, A. N., *et al.* 2018, *Astron. J.*, **156**, 241.

Kochanek, C. S., *et al.* 2017, *Publ. Astron. Soc. Pacific*, **129**, 104502.

Lenz, P., and Breger, M. 2005, *Commun. Asteroseismology*, **146**, 53.

Paunzen, E., and Vanmunster, T. 2016, *Astron. Nachr.*, **337**, 239.

Rodriguez, E., Gonzalez-Bedolla, S. F., Rolland, A., Costa, V., and Lopez de Coca, P. 1997, *Astron. Astrophys.*, **324**, 959.

Shappee, B. J., *et al.* 2014, *Astrophys. J.*, **788**, 48.

Stassun, K. G., *et al.* 2019, *Astron. J.*, **158**, 138.

Zhou, A.-Y., *et al.* 2017, arXiv:1710.03944.